ACS OMEGA

http://pubs.acs.org/journal/acsodf Article

Study of Reasonable Grouting Pressure in the Process of Measuring Coal Seam Gas Pressure and Application

Fengfeng Yang,* Xiangjun Chen, Jufeng Zhang, and Jinkui Ma

Cite This: *ACS Omega* 2023, 8, 25892−25902 Read Online

ACCESS | Metrics & More | Article Recommendations

ABSTRACT: Coal seam gas pressure is an important index to evaluate the risk of coal outbursts. The accuracy of measurement is closely related to the quality of hole sealing, and reasonable grouting pressure is one of the key factors to determine the quality of hole sealing. To obtain a reasonable grouting pressure, a mathematical model for slurry flow was established based on the relationship between the seepage law of the slurry and the properties of the borehole surrounding a rock. According to the conditions of the working face 11111 of the coal seam Ji_{15-17} in Pingdingshan No. 13 Coal Mine, the reasonable grouting pressure in the process of hole sealing and pressure measurement were simulated by COMSOL multiphysics numerical simulation software. After comparing the pressure distribution and slurry diffusion characteristics in the borehole under different grouting pressures, it is concluded that the reasonable grouting pressure is 4 MPa. When 4 MPa grouting pressure to seal the hole is used during actual engineering verification, the measured gas pressure is 2.7 MPa, which is more accurate than the result obtained under conditions of sealing with normal pressure grouting.

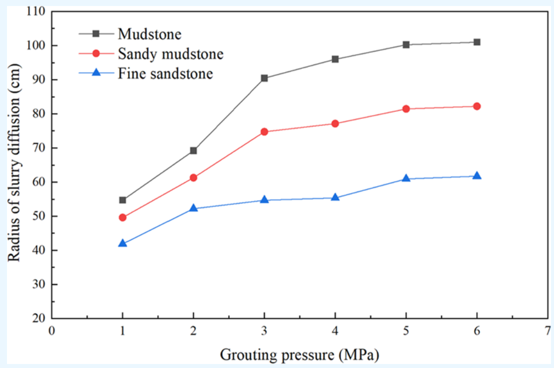

1. INTRODUCTION

Coal resources have always been the basic energy supporting economic development in China.[1] In recent years, with the deepening of mining depth and the increasing complexity of coal mining, the deep coal seams have generally exhibited high ground stress, high gas content, and high gas pressure characteristics. Gas disasters have become one of the factors seriously affecting mine safety production.[2,3] Gas pressure is an important indicator for preventing gas disasters, which directly reflects the gas content in coal seams and the potential danger level of coal and gas outbursts.[4−6] However, accurate measurement of coal seam gas pressure is very difficult under complex production conditions.[7,8] According to the long-term experience in coal seam gas pressure measurement, the success rate can reach as high as 70%.[9] Low success rate and inaccuracy of measurement will increase the danger in production, which limits the production speed of the mine. Therefore, accurate determination of gas pressure in a coal seam is of great significance for gas control in mines.

At present, pressure measurement methods are generally divided into direct and indirect.[10,11] When using the direct measurement method, the key is hole sealing. According to different sealing materials, common sealing methods include mud sealing, cement mortar sealing, rubber ring sealing, polyurethane foam sealing,[12] etc. Considering the quality, cost, and difficulty of the sealing process, grouting sealing is the most widely used method up to now.[13] However, its disadvantage is that when the hole sealing segment is in the soft rock or there are microcracks around the drilling hole, or when the pressure measurement drilling hole is constructed directly in the coal seam, good sealing quality cannot be guaranteed, and the sealing section is prone to gas leakage, resulting in the outcome lower than the actual one. To overcome this disadvantage, scholars have proposed a "two sealing and one injection" pressure grouting hole sealing process,[14] which can seal the cracks around the drilling hole by injecting slurry. Then, the expansion force of the solidified grouting material can approach the ground stress, which makes the borehole sealing section form a high-stress zone. This reduces the air leakage channels and improves the sealing performance.[15]

In order to improve the quality of hole sealing, scholars have conducted extensive research on sealing material and technology. Yu et al.[16] put forward the solid−liquid sealing technology of "three plugging and two injection" and developed the sealing device and materials. Xiong et al.[17] tested three different sealing technologies, namely, bagged polyurethane sealing, self-expanding sealing device, and new-type expansive cement sealing. It is found that the new-type expansive cement has the

Received: March 9, 2023
Accepted: June 28, 2023
Published: July 14, 2023

best sealing effect especially on coal cracks. Chao et al.[18] analyzed the deformation, strength characteristics, and pore evolution of three sealing materials through a triaxial compression test and nuclear magnetic resonance test. The results show that the increase in the elastic modulus and deformation modulus of sealing materials under confining pressure is proportional to those at low confining pressure. Qin et al.[19] established a chance selection model for secondary sealing when the sealing of some boreholes is damaged under advanced support pressure and developed a dynamic secondary sealing device. Song et al.[20] studied the instability characteristics of the borehole sealing section in view of the instability and sealing difficulties faced by the soft coal seam gas drainage borehole. Scholars have also carried out some research studies on numerical simulation. Zhang et al.[21] used the COMSOL numerical simulation method to analyze the influence of fissure angle and initial water flow velocity on slurry diffusion, and the changes of the pressure field, velocity field, and water flow during slurry diffusion in inclined fractures. Zhao et al.[22] addressed the problem of low gas extraction efficiency in low-permeability coal seams by using numerical simulation to compare the gas extraction efficiency of different sealing lengths and determined the appropriate sealing length for gas extraction boreholes. Scholars study grouting through not only field engineering but also through similar experiments. Zhang et al.[23] adopted the regional advanced grouting technology to prevent water inrush from the karst aquifer in the coal seam floor and, based on the Bernoulli's equation, established the relationship of pressure between the ground and the critical grouting. Zhang et al.[24] used the 1:20 geometric similarity ratio indoor model to simulate the grouting experiment and applied the soil pressure and pore water pressure sensor to study the pressure response of the surrounding sand layer to the inclined shaft grouting. Ma et al.[25] obtained the relationship between the grouting pressure and compressive strength of cement slurry through experimental research. However, existing research rarely link the grouting pressure with the sealing effect directly, and in engineering practice, the selection of grouting pressure is still founded on previous experience instead of sufficient scientific basis.

In the current pressure testing of pressurized sealing holes, it is generally believed that the grouting pressure needs to be above 8.0 MPa to effectively seal the rock fractures around the borehole. However, the reasonable pressure is not fixed in practical engineering. In order to determine the reasonable grouting pressure under specific surrounding rock conditions, this paper analyzes the influence of surrounding rock structure characteristics on the grouting effect by combining the rock lithology at the pressure measuring site of Pingdingshan No. 13 Coal Mine and the rock mass physical and mechanical properties. Considering the different lithology around the boreholes, the slurry diffusion radius under distinct grouting pressures is studied by numerical simulation, and a reasonable grouting pressure is selected, which can provide experience in grouting and hole sealing for mines with similar geological and gas occurrence conditions.

2. METHODS

Based on the diffusion model of slurry in the stratum and the actual situation of grouting, COMSOL software is used to simulate the pressure distribution formed by the cement slurry seepage after grouting in the rock drilling, from which we can analyze the influence of grouting pressure on the slurry diffusion range, obtain the slurry diffusion distance under different grouting pressures, and then determine the reasonable grouting pressure.

2.1. Plastic Zone of Borehole. When the borehole is excavated, a crushing ring will form around the borehole due to the disturbance of the drill pipe to the surrounding coal. The fissure of the crushing ring is well developed. If the slurry cannot fill the whole range, the poor hole sealing quality will lead to gas leakage and failure of gas pressure measurement. Due to the relatively difficult field measurement, the borehole plastic zone is simulated by the numerical simulation method. Since the borehole length is much longer than that of the diameter, the stress on the borehole wall can be considered as a plane strain problem.

To obtain the radius of the crushing ring around the borehole, the following basic assumptions are made:

(1) The coal is a homogeneous and isotropic continuous medium.
(2) The stress distribution around the borehole is shown in Figure 1.

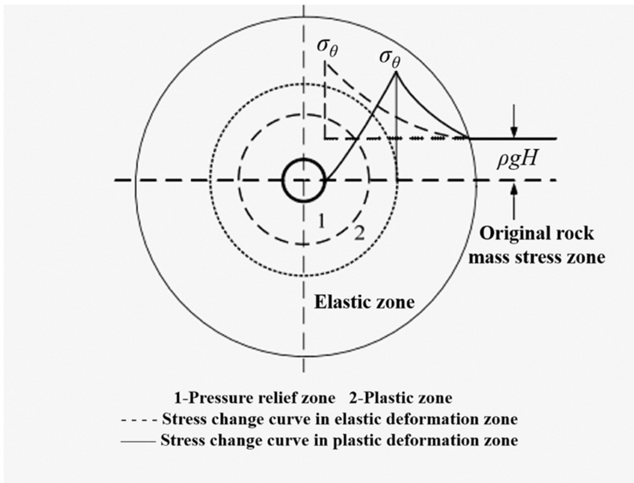

Figure 1. Stress distribution around the borehole.

(3) The stress distribution in the elastic zone is the same as that around the stressed circular hole in the elastic body, and the deformation of rock mass in the plastic zone meets the Mohr−Coulomb yield criterion.
(4) The rock stress in the crushing ring is less than that of the original one.

Based on the above assumptions, the radius of the plastic zone and the radius of the crushing zone can be obtained:[26]

The radius of the plastic zone is

$$R = a\left[\frac{(p + c\cot\varphi)(1 - \sin\varphi)}{p_i + c\cot\varphi}\right]^{1-\sin\varphi/2\sin\varphi} \tag{1}$$

The radius of the crushing area is

$$R_s = a\left[\frac{(p + c\cot\varphi)(1 - \sin\varphi)}{(1 + \sin\varphi)(p_i + c\cot\varphi)}\right]^{1-\sin\varphi/2\sin\varphi} \tag{2}$$

where R is the radius of the plastic zone, m; P is the original rock stress, MPa; φ is the internal friction angle, °; a is the drilling radius, m; and c is the cohesion.

https://doi.org/10.1021/acsomega.3c01601
ACS Omega 2023, 8, 25892−25902

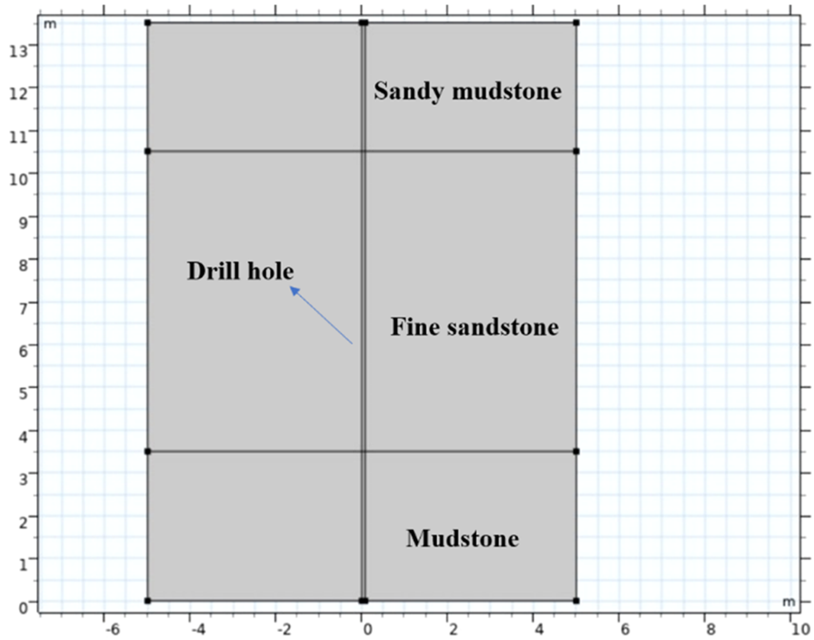

Figure 2. Model of numerical simulation.

It can be seen from the above formula that the borehole stability and surrounding displacement mainly depend on the original stress, borehole radius, internal friction angle, cohesive force, and other factors of the rock stratum. With the increase of borehole radius, both the plastic zone radius and the peripheral displacement increase, while the peripheral displacement of the plastic zone increases significantly with the decrease of internal friction angle and cohesion.

2.2. Mathematical Model of Slurry Diffusion. *2.2.1. Basic Assumptions.* There are many factors that affect the pressure measurement. In order to simplify the problem in the actual research, the following assumptions are made for the mathematical model when studying the reasonable grouting pressure:

(1) The seepage movement of slurry in the rock stratum is subject to Darcy's law.
(2) The grout only seeps and diffuses in the crack of the surrounding rock of the grouting section.
(3) The injection pressure of drilling slurry is approximately equal to the control pressure in the orifice grouting pump.
(4) The rock stratum of the grouting section is homogeneous and isotropic.
(5) The grout is an incompressible fluid.

Mathematical models:

(1) Basic seepage law: fluid motion in porous medium conforms to Darcy's law:[27]

$$\nu = -\frac{k}{\mu}(\nabla P + \rho g \nabla D) \tag{3}$$

where ν is the seepage velocity, m/s; k is the permeability, m^2; μ is the dynamic viscosity, $kg{\cdot}(m{\cdot}s)^{-1}$; P is the fluid pressure, $kg/(m{\cdot}s^2)$; ρ is the slurry density, $kg{\cdot}m^{-3}$; g is the gravitational accelerations, $kg{\cdot}m^{-3}$; and D is the vertical coordinates (such as x, y, z).

(2) The continuity equation of slurry seepage in rock mass:[28]

$$\frac{\partial(\rho\phi)}{\partial t} + \nabla(\rho\nu) = \rho q \tag{4}$$

where φ is the porosity; q is the fluid volume, source and sink strength; and t is the time, s.

In the numerical simulation of fluid seepage, the fluid seepage velocity is secondary. The relationship between pressure P and density ρ is obtained by combining Darcy's law with continuity equation of slurry seepage. The following formulas can be obtained from (3) and (4)

$$\frac{\partial(\rho\phi)}{\partial t} + \nabla{\cdot}\rho\left[-\frac{k}{\mu}(\nabla P + \rho g \nabla D)\right] = \rho q \tag{5}$$

For incompressible fluids, the density is constant, and the above formula can be simplified as

$$\frac{\partial(\phi)}{\partial t} + \nabla\left[-\frac{k}{\mu}(\nabla P + \rho g \nabla D)\right] = q \tag{6}$$

(3) Grouting seepage control equation

$$S\frac{\partial P}{\partial t} + \nabla\left[-\frac{k}{\mu}(\nabla P + \rho g \nabla D)\right] = q \tag{7}$$

where S is the storage coefficient, MPa^{-1}.

2.2.2. Numerical Model and Boundary Conditions. 2.2.2.1. Establishment of Numerical Model. The grouting hole sealing for testing gas pressure is a three-dimensional problem, considering the feasibility and effectiveness of numerical calculation, the problem should be simplified, the radial direction of pressure measurement borehole is selected for modeling, and the three-dimensional problem is transformed to a two-dimensional problem.

Combined with the surrounding rock properties of the test site for pressure measurement, the model is established as follows: Taking the geometric center of the borehole as the center, the diameter of the borehole is 0.075 m, the sealing section involves three kinds of rocks, and the length of the

https://doi.org/10.1021/acsomega.3c01601
ACS Omega 2023, 8, 25892−25902

grouting section passing through mudstone, fine sandstone, and sandpaper mudstone is 3.5, 7, and 3 m, respectively.

The slurry diffusion radius is set to 30, 25, 20, 15, 10, and 5 m for simulation, and the results show that the diffusion radius is less than 2 m. In order to make the simulation results clearer, the model size is represented by 5 m from the calculation model boundary to the borehole wall. The simulation model is shown in Figure 2. Due to the deformation of the surrounding rock caused by roadway excavation, the porosity of the surrounding rock will change. Combined the integrity of the surrounding rock of mine roadway and other conditions, it is assumed that the porosity of the three rocks has increased to varying degrees after being damaged. The porosity, permeability, and other relevant parameters after the change are shown in Table 1.

Table 1. Related Parameters of the Numerical Simulation

variable	description	unit	value
g	gravitational acceleration	$m{\cdot}s^{-2}$	9.80
density	density of slurry	$kg{\cdot}m^{-3}$	1280
μ	slurry viscosity coefficient	Pa·s	$2.8e^{-4}$
kappa-xsy	permeability of fine sandstone	m^2	$1.7e^{-13}$
kappa1-ny	permeability of mudstone	m^2	$8.7e^{-19}$
kappa1-sny	permeability of sandy mudstone	m^2	$1.2e^{-16}$
fract-ny	porosity of mudstone	%	3.4%
fract-xsy	porosity of fine sandstone	%	5.3%
fract-sny	porosity of sandy mudstone	%	4.4%

2.2.2.2. Initial and Boundary Conditions. Take the borehole boundary as the slurry inflow boundary of the grouting section, and there is no slurry flow at other boundaries. The initial condition is

$$P|_{t=0} = P_0 \tag{8}$$

where P_0 is the initial pressure at the borehole boundary of grouting.

The slurry pressure gradient is 0 at infinity. The boundary condition of the model is

$$\begin{cases} P|_{r=0} = P_0 \\ \left.\dfrac{\partial P}{\partial r}\right|_{r=l} = 0 \end{cases} \tag{9}$$

3. RESULTS AND ANALYSIS

3.1. Influence Range of Plastic Borehole Zone. Taking the drilling operation in fine sandstone as an example, a two-dimensional plane model is established to analyze the variation law of the plastic zone and the stress around the borehole. The upper is covered by a rock mass of 600 m (average density is 2500 $kg{\cdot}m^{-3}$), that is, the upper load is 15 MPa, and the left, right, and lower parts are sliding boundaries. The simulation results are as follows:

It can be seen from Figures 3 and 4 that the surrounding rock stress changes after the formation of the borehole, in which the tensile stress is positive and the compressive stress is negative. As we can see from the horizontal strain nephogram, the horizontal stress around the borehole decreases along both sides and increases along the up and down directions, while the vertical stress increases along both sides and decreases along the upper and lower directions.

As shown in Figures 3a and 4a, around the borehole, the tensile strain occurs, and the formed pressure relief space aggravates the stress imbalance, resulting in some deformation and damage. As shown in Figure 5, the red area is the plastic failure area, and the failure range is about 30 mm. In the plastic zone, the surrounding rock fractures develop, providing more channels for gas flow, reducing the effectiveness of hole sealing, which is one of the most difficult problems to be overcome in the pressure measurement. Therefore, the plastic zone must be sealed tightly.

3.2. Pressure Distribution under Different Grouting Pressures. The pressure distribution nephogram of slurry seepage under different grouting pressures is shown in Figure 6.

The results of the simulation are as follows:

(1) When the lithology around the borehole is mudstone, sandy mudstone, or fine sandstone, under the same grouting pressure, the pressure distribution of slurry seepage in different rock layers is different, that is to say, the slurry diffusion radius is different in different lithology; the radius in fine sandstone is the largest, followed by sandy mudstone, with mudstone having the smallest radius. Under different grouting pressure, the diffusion in the same surrounding rock is also different, which is difficult in mudstone and easy in fine sandstone.

(2) The seepage of slurry at the boundary of two different rock layers is relatively easy because the porosity and

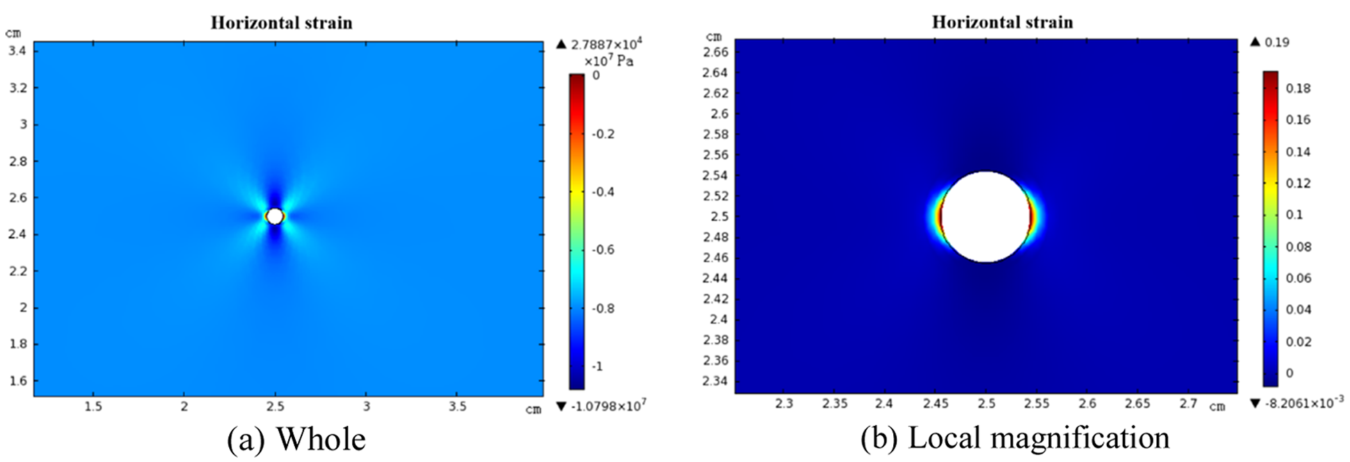

Figure 3. Horizontal stress changes after the formation of a borehole.

https://doi.org/10.1021/acsomega.3c01601
ACS Omega 2023, 8, 25892−25902

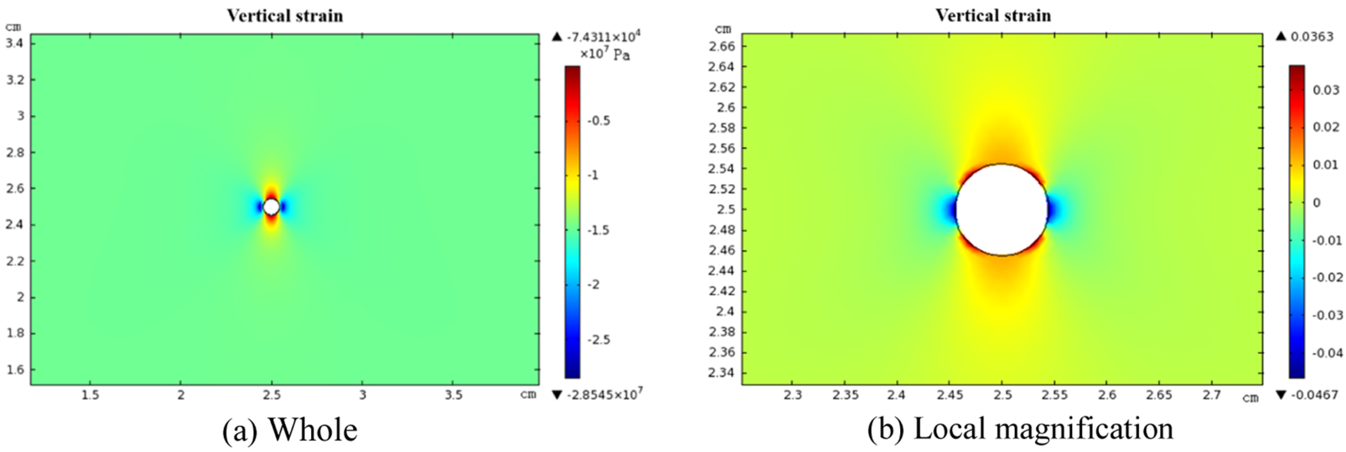

Figure 4. Vertical stress map after the formation of a borehole.

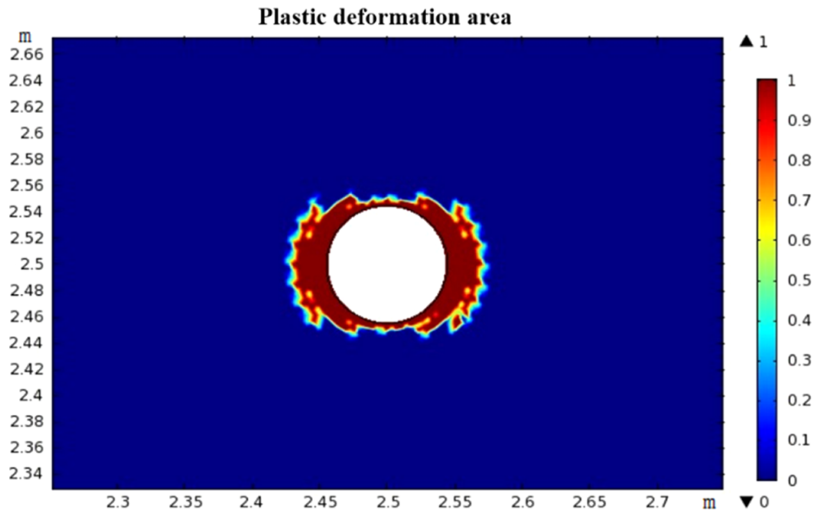

Figure 5. Plastic damage area around the borehole.

permeability between the two rock layers change greatly, and the cracks are more developed for seepage diffusion.

(3) When the grouting pressure is constant, the pressure distribution law of the same rock layer around the borehole is the same, and the pressure distribution is independent of the length of the borehole. The pressure decreases only in the radial direction of the borehole until the slurry pressure decays to be equal to the pore pressure, and the slurry keeps still. The maximum distance between the slurry and the borehole wall is the diffusion radius of the slurry.

(4) For the same rock, when the grouting pressure is less than a certain range, the increase of slurry diffusion radius is obvious with the growth of grouting pressure. When the grouting pressure continues to ascend and exceeds a certain spot, the increasing trend of radius is not conspicuous. In different rock layers, the grouting pressure required for the slurry to reach the same diffusion radius is also different. Therefore, the reasonable grouting pressure is distinct for different surrounding rocks to achieve the best sealing.

3.3. Slurry Diffusion Characteristics under Different Grouting Pressures. Based on the simulation results of slurry pressure distribution under different grouting pressures, COMSOL multiphysics software was used to extract data, and the law of slurry pressure attenuation with diffusion radius under the same grouting pressure was studied. The general rule is as follows: the slurry pressure will gradually decline due to overcoming the flow resistance when flows. The farther away from the borehole wall, the smaller the slurry pressure is, as shown in Figure 7.

(1) According to Figures 6 and 7, the diameter of the borehole is 75 mm, so the distance between the borehole boundary and the borehole center is 37.5 mm. The maximum grouting pressure point during diffusion is located by 37.5 mm away from the borehole center, that is, the maximum grouting pressure point is the borehole wall, and the grouting pressure continues to decay outward with the borehole as the center. The decay rate is related to the surrounding rock properties and in situ stress around the borehole. With the seepage and diffusion of slurry, the grouting pressure decreases in varying degrees until it is equal to the pore pressure, and the slurry stops to flow. The maximum distance between the slurry seepage and the borehole wall is the slurry diffusion radius.

(2) When the grouting pressure is constant, the slurry diffusion in fine sandstone, mudstone, and sandy mudstone is different. When the grouting pressure reaches 6 MPa, the diffusion distance of slurry in fine sandstone is more than 975 mm, while in mudstone, it is

https://doi.org/10.1021/acsomega.3c01601
ACS Omega 2023, 8, 25892−25902

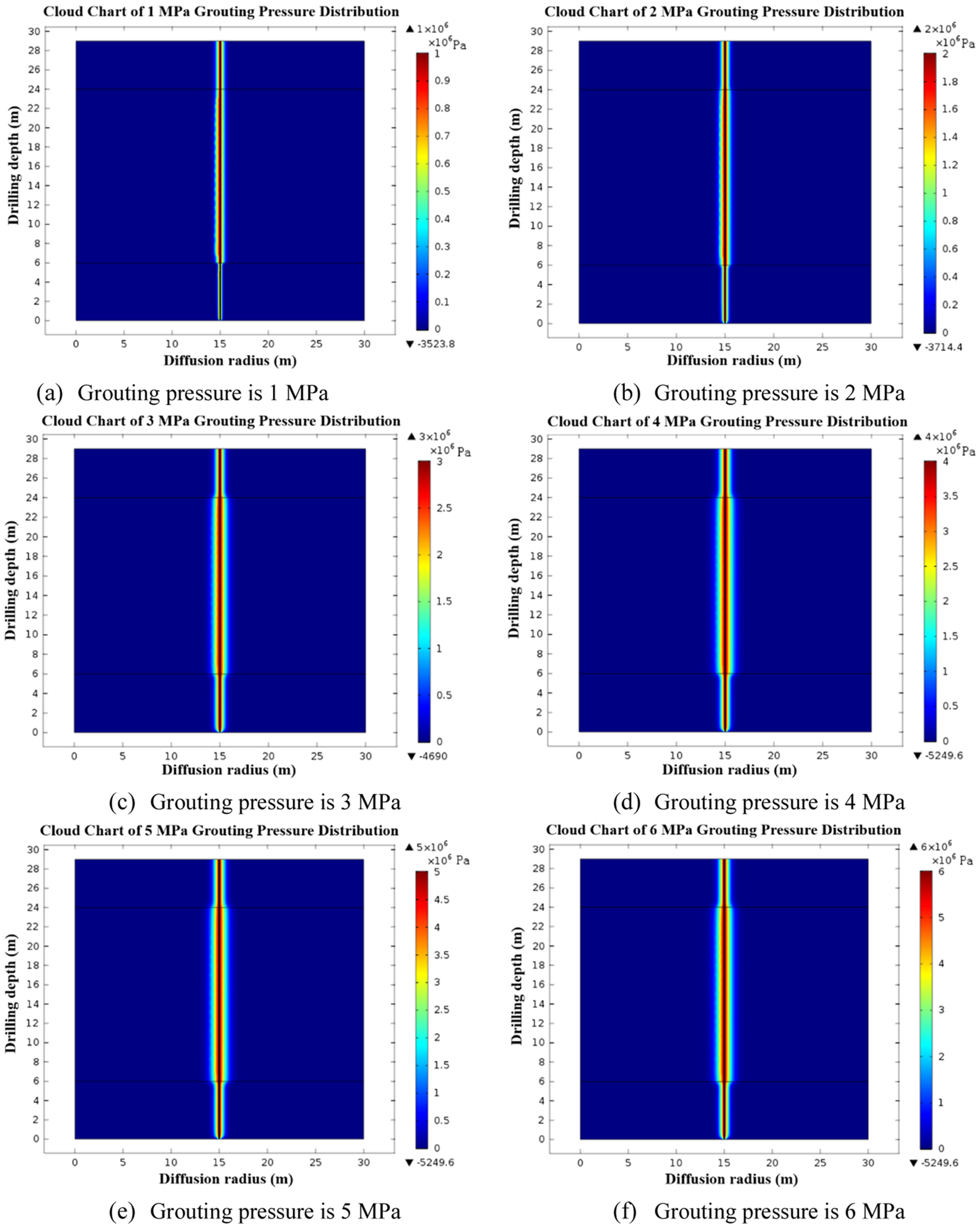

Figure 6. Slurry pressure distribution under different grouting pressures.

only about 575 mm. It can be seen from Figure 7 that the diffusion distance of slurry in fine sandstone is the largest, followed by sandy mudstone, and the diffusion distance in mudstone is the smallest. Due to the different lithology of the three surrounding rocks, the permeability, porosity, and fracture development degree, the hardness of the

https://doi.org/10.1021/acsomega.3c01601
ACS Omega 2023, 8, 25892−25902

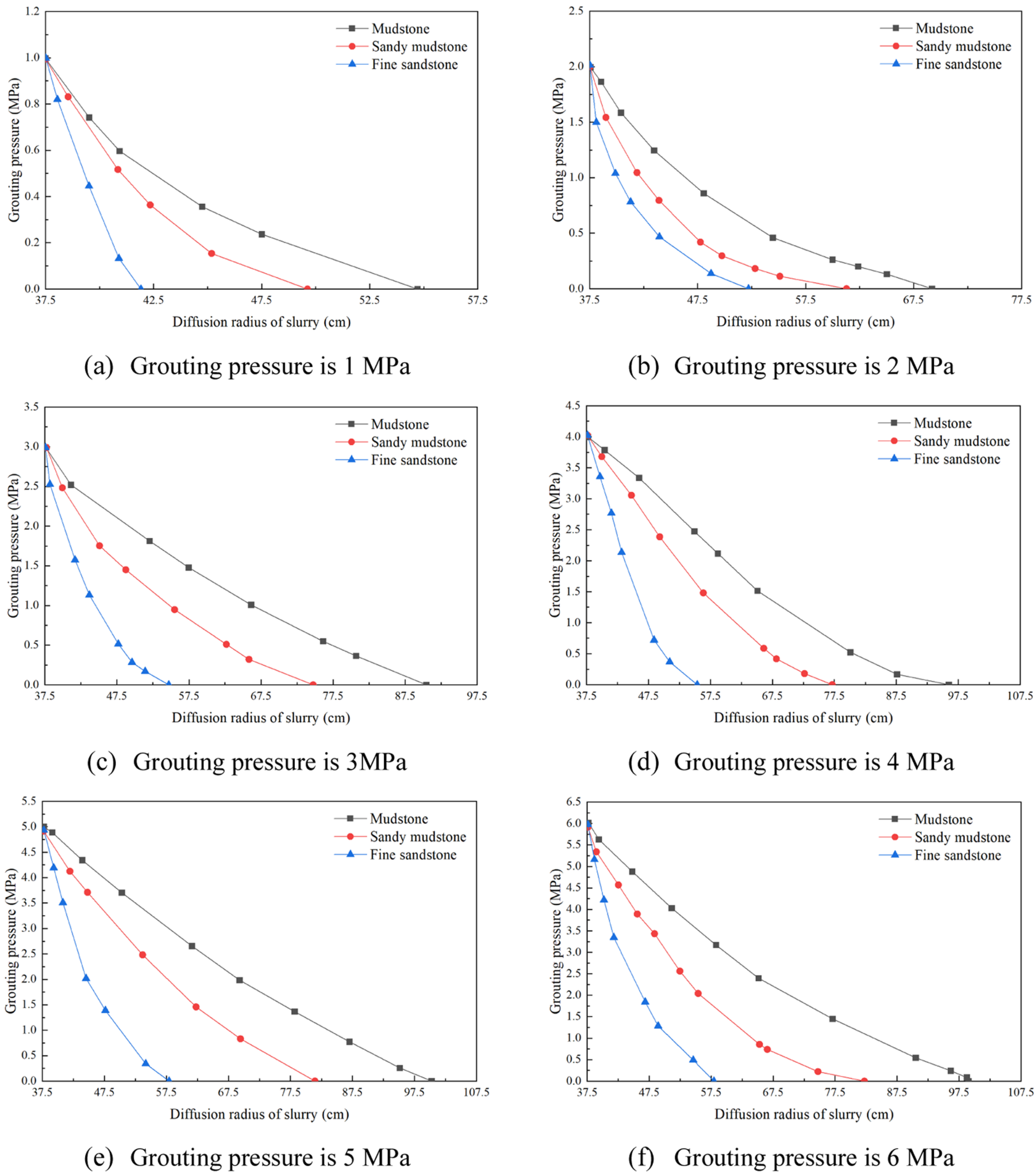

Figure 7. Attenuation diagram of grouting pressure with diffusion radius.

surrounding rock, and in situ stress are also different. The greater the permeability is, the higher the porosity and fracture development degree is, and the lower the firmness coefficient of the surrounding rock, the easier the slurry diffuses. Therefore, the grouting pressure is affected by geological conditions, and different hole sealing technologies and corresponding grouting pressure should be selected under different geological conditions.

(3) For a certain kind of rock stratum, the grout diffusion distance increases with the increase of grouting pressure, so the grouting pressure plays a key role in the seepage diffusion of grout.

3.4. Determination of Reasonable Grouting Pressure.

In order to analyze the reasonable grouting pressure, extract the corresponding slurry diffusion radius data when the grouting pressure attenuation is zero, and generate the curve illustrating

https://doi.org/10.1021/acsomega.3c01601
ACS Omega 2023, 8, 25892−25902

the relationship between grouting pressure and diffusion distance, as shown in Figure 8.

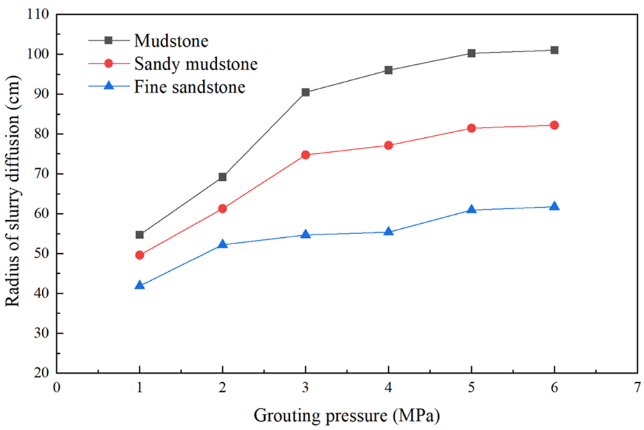

Figure 8. Grout diffusion radius under different grouting pressures.

It can be seen from Figure 8:

(1) The diffusion radius of grout in rock formation is positively correlated with the grouting pressure. With the increase of grouting pressure, the diffusion radius of grout gradually increases, but when the pressure is up to a certain value, the rising trend of radius is not obvious. At this time, it is unreasonable to increase the grout diffusion radius by continuously increasing the grouting pressure because the main factor affecting the grout diffusion radius is the nature of the surrounding rock, and the rock stratum has a limit pressure that it can withstand. When the grouting pressure is higher than the limit, the rock mass will split, forming a large number of new flow channels, resulting in poor sealing effect or even failure.

(2) When the grouting pressure of fine sandstone, sandy mudstone, and mudstone is less than 4, 3, and 2 MPa, respectively, with the increase of grouting pressure, the slurry diffusion rate is very fast, and the ascending trend of diffusion radius is obvious. When the grouting pressure of fine sandstone, sandy mudstone, and mudstone is greater than 4, 3, and 2 MPa, respectively, with the increase of grouting pressure, the increasing slows down. When the pressure continues to increase, the variation of the radius is very small, which indicates that the grouting pressure no longer plays a leading role in the formation of slurry diffusion radius. In addition, the slurry diffusion distance is greater than the radius of the plastic zone of the borehole, that is, the slurry can block the entire plastic zone. Therefore, it can be considered that the reasonable grouting pressure is 4 MPa.

4. ENGINEERING VERIFICATION

4.1. Engineering Background. The pressure measurement site is selected at the rock roadway on the floor of the machine roadway of working face 11111 in the coal seam Ji_{15-17}, with the section of 15.20 m^2. The working face 11111 in the coal seam Ji_{15-17} is located in the sixth section of the east wing of the No. 1 mining area, which tends to the safety coal pillar as the east boundary, the west is the protection coal pillar of the east air shaft, the south is the working face 11131 in the coal seam Ji_{15-17} that has not been mined, and the north is the working face 11091 in the coal seam Ji_{15-17} that has been mined. The ground is located in Baopo and Yuzhuang, with ground elevation by +80−85 m and working face elevation by − 470 to − 630 m. The occurrence is relatively stable, with a thickness of 4.35−6.20 m, an average of 5.80 m, a dip angle of 10−19°, a strike of 80−100°, and a dip of 170−190°. The direct roof of the coal seam is sandy mudstone with a thickness of 0.6−2.6 m, the main roof is fine- and medium-grained sandstone (thickness: 1.2−8.1 m), the direct bottom is sandy mudstone of 0.2−3.5 m, and the main bottom is 4.7−9.4 m fine sandstone and sandstone interbedding. Because the roof and floor of the coal seam are sandy mudstone, the permeability is poor. Most of the exposed rock strata in the floor rock roadway are interbedded with fine sandstone and sandy mudstone in the range of 1/3−1/4 at the upper right of the roadway, which are grayish black, and the rest are mudstone.

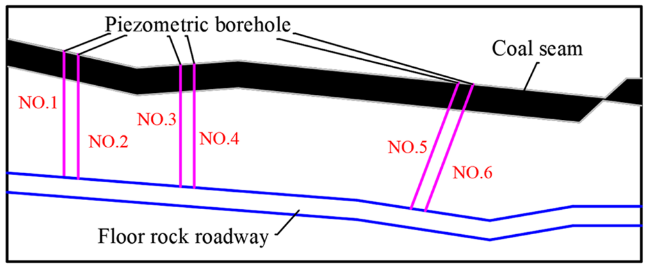

Figure 9. Specific location of pressure measuring borehole.

According to the geological structure, surrounding rock state, and the layout of extraction holes, the specific positions of three pressure measuring fields are determined. The first pressure measuring field is of 380 m from the outer opening of the roadway, and the pressure measuring holes 1 and 2 are arranged in the field. The normal staggered distance of the two pressure measuring hole openings in the roadway should be greater than 1.0 m, and the axial staggered distance should be greater than 2.0 m. Therefore, No. 3 and No. 4 holes are selected at 405 and 410 m away from the outside of the roadway, respectively. The second field should be more than 25 m apart from the first one, and the distance from the fault should exceed 30 m. Therefore, No. 3 and No. 4 holes are selected at 405 and 410 m away from the outside of the roadway, respectively. The third field locates between the two fault layers with the relatively complete section. The distance between No. 5 and No. 6 pressure measuring holes and the outer opening of the roadway is 450 and 455 m, respectively. The specific location of the pressure drilling hole is shown in Figure 9.

According to the site, the locations of the test boreholes were determined. There were three pressure measuring fields, and each field was equipped with two boreholes. No. 1, No. 3, and No. 5 boreholes are arranged on the left side of the roadway, and No. 2, No. 4, and No. 6 on the right. See Table 2 for the parameters of pressure measurement borehole.

4.2. Results and Analysis of Pressure Measurement. In No. 1 borehole, a bag is used to block the orifice of the borehole, and the hole sealing is conducted under normal pressure. While No. 2−6 boreholes, the pressure grouting method is used to seal the hole, and the grouting pressure is 4 MPa. The hole sealing method is "two blocking and one injection" bag sealing method, and the CPD8M type coal seam gas pressure automatic tester is used to measure the gas pressure. The results measured are shown in Table 2. The gas pressure recovery curve of boreholes 1−6 is shown in Figure 10.

https://doi.org/10.1021/acsomega.3c01601
ACS Omega 2023, 8, 25892−25902

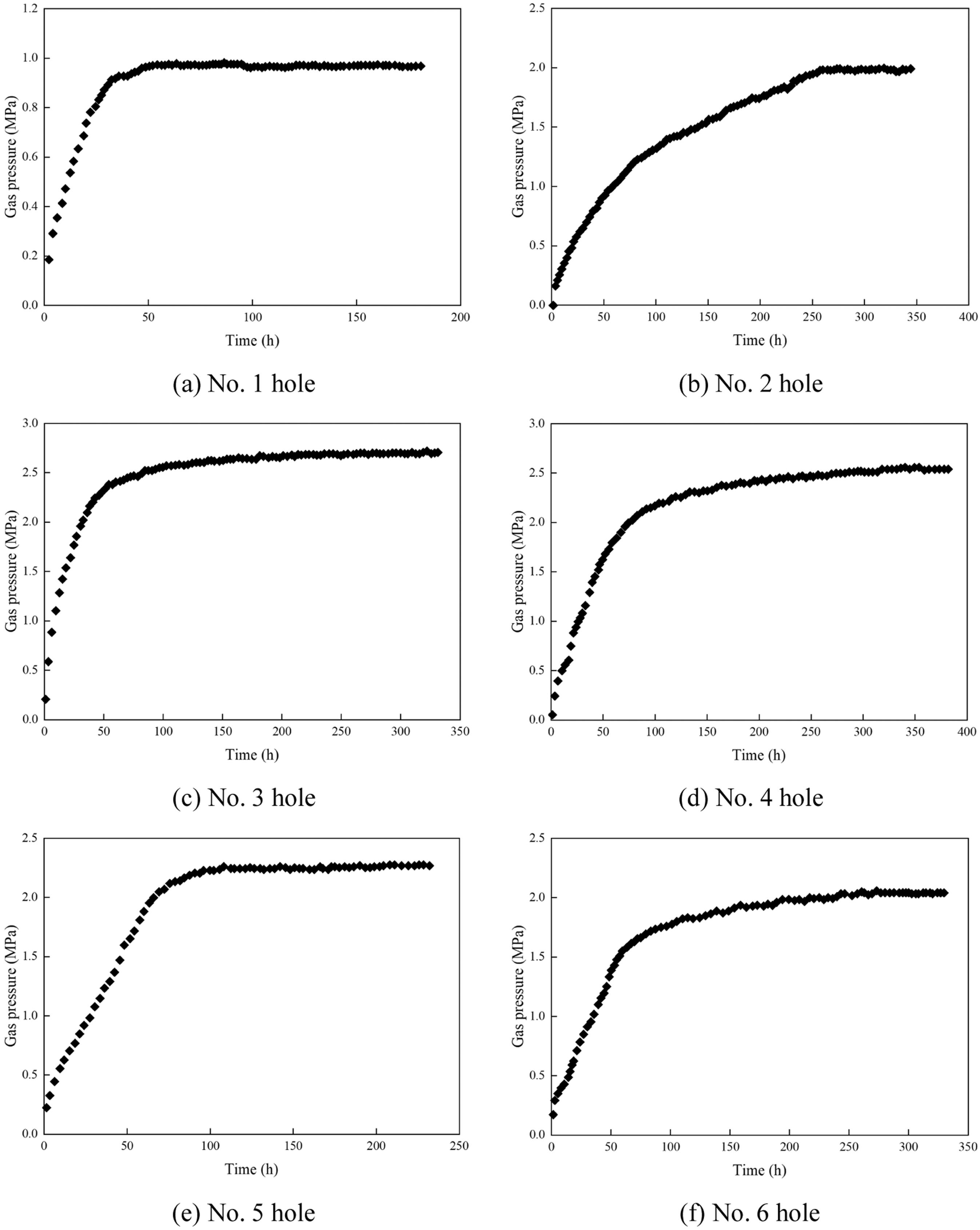

Figure 10. Gas pressure recovery curve of boreholes.

(1) It can be seen from Figure 10 that the curve conforms to the characteristics of coal seam gas pressure recovery, which indicates that the measured pressure does not include water pressure, and no water is found in the borehole during on-site pressure measurement, which is consistent with the engineering practice.

https://doi.org/10.1021/acsomega.3c01601
ACS Omega 2023, 8, 25892−25902

Table 2. Parameters of Borehole Layout and Test Results of Gas Pressure

number	distance from roadway outer opening (m)	aperture (mm)	hole length (m)	depth of sealing hole (m)	angle (°)	Azimuth (°)	gas pressure (MPa)
1	380	75	41.9	29.0	30	194	0.97
2	385	75	39.3	31.0	52	194	1.97
3	405	75	41.9	29.0	30	194	2.70
4	410	75	39.3	33.5	52	194	2.54
5	450	75	40.9	29.5	30	194	2.30
6	455	75	42.6	31.5	52	194	2.02

(2) No. 1 and No. 2 boreholes are in the same drill site, which exists no influence of geological structure and groundwater, and the coal seam occurrence conditions are the same. No. 1 borehole was sealed by atmospheric pressure grouting, and the measured gas pressure is 0.97 MPa. The "two plugging and one injection" bag type hole sealing method is adopted in No. 2, and the grouting pressure is 4 MPa, the measured pressure is 1.97 MPa, which is 1.0 MPa higher than the gas pressure measured in borehole No. 1. The "two plugging and one injection" bag type hole sealing method with a grouting pressure of 4.0 MPa was adopted for the No. 3—No. 6 boreholes in other sites, and the results were also much higher than 0.97 MPa. It can be considered that the pressure measurement result of grouting hole sealing with a grouting pressure of 4.0 MPa is more accurate than that of the normal, which shows that under the same other conditions, the grouting pressure plays a key role in hole sealing.

In summary, it is reasonable to select a grouting pressure of 4 MPa and which can meet the requirements under this condition. Moreover, the technology, characterized by "two plugs and one injection" bag type rapid sealing automatic pressure measurement, can be fully applied to the measurement of coal seam gas pressure under the same conditions.

5. DISCUSSION

Based on Darcy's law and the continuity equation of grout seepage in rock mass, the grouting seepage control equation and grouting model are established. Compared with the existing research, the slurry model constructed in this paper simplifies the slurry flow as a two-dimensional problem, and regards the velocity as a non-important factor, while focusing on the pressure. This model is simple and effective for this paper. Through simulation calculation, the variation law of grout diffusion radius in surrounding rock under different grouting pressure is obtained, and the most reasonable grouting pressure is determined to be 4 MPa. Through numerical simulation analysis, it was found that the plastic failure zone of the borehole is around 30 mm, and under a grouting pressure of 4 MPa, the minimum diffusion radius of the slurry is 550 mm. This indicates that effective sealing of the plastic zone of the borehole can be achieved under a grouting pressure of 4 MPa. Tests were also carried out at the project site, the measured gas pressure under 4 MPa grouting pressure is more accurate than that under normal pressure, which also verifies the effectiveness of the model. Compared with previous studies, this study links the grouting pressure with the grouting effect, and the research results are extensive and can provide theoretical reference for grouting engineering under similar surrounding rock and geological conditions. However, there are also certain limitations, as the surrounding rock conditions of mines are different. Overall, this study provides a method for determining reasonable grouting pressure.

6. CONCLUSIONS

In this work, a mathematical model of grout seepage is established derived from Darcy's law and the seepage law of grout in the rock mass, and a two-dimensional grouting model is also established based on the geological properties of the test site.

Combining the specific geological conditions of the test working face with simulating the stress change in the plastic zone around the borehole, it is determined that the damage range around the borehole is about 30 mm. The horizontal stress around the borehole decreases in the horizontal direction and increases in the vertical direction. The vertical stress around the borehole increases in the horizontal direction and decreases in the vertical direction.

By simulating the diffusion characteristics of grout under different grouting pressures, it is concluded that the critical grouting pressure for fine sandstone, mudstone, and sandy mudstone is 4, 3, and 2 MPa, respectively. Since the drilling is composed of three types of rock, the reasonable grouting pressure is 4 MPa. At which, the diffusion radius of slurry is far greater than the influence range of the borehole plastic zone, and the borehole can be effectively sealed. Through practical engineering verification, it is found that when the grouting pressure is 4 MPa, the highest gas pressure in the tested coal seam is 2.7 MPa, which is more accurate than the pressure test results obtained from normal pressure grouting sealing. Therefore, it is reasonable to determine the grouting pressure as 4 MPa.

■ AUTHOR INFORMATION

Corresponding Author

Fengfeng Yang − *College of New Energy, Longdong University, Qingyang 745000, China*; orcid.org/0000-0002-3939-2297; Email: yangff1107@mail.ustc.edu.cn

Authors

Xiangjun Chen − *State Key Laboratory Cultivation Base for Gas Geology and Gas Control (Henan Polytechnic University), Jiaozuo 454003, China*; orcid.org/0000-0003-4849-8349

Jufeng Zhang − *College of New Energy, Longdong University, Qingyang 745000, China*

Jinkui Ma − *China Coal Technology & Engineering Group, Fushun 113122, China*

Complete contact information is available at: https://pubs.acs.org/10.1021/acsomega.3c01601

Notes

The authors declare no competing financial interest.

■ ACKNOWLEDGMENTS

This research was supported by the Youth Science and Technology Foundation of Gansu Province (22JR5RM213), the University Innovation Foundation of Gansu Province

(2021B-278), the Natural Science Foundation of Gansu Province (21JR11RM049), and the Science and Technology Program of Qingyang (QY2021A-F025).

■ REFERENCES

(1) Teng, X.; Liu, F.; Chiu, Y. The Impact of Coal and Non-Coal Consumption on China's Energy Performance Improvement. *Nat. Resour. Forum* **2020**, *44*, 334−352.

(2) Wang, F.; Zhang, P.; Cui, B.; Sun, Z.; Zhang, K. Research Progress of Disaster Factors and a Prevention Alarm Index of Coal and Gas Outbursts. *Arab. J. Geosci.* **2021**, *14*, 2042.

(3) He, L.; Dai, Y.; Xue, S.; Zheng, C.; Han, B.; Guo, X. Study on Gas Control Methods Optimization for Mining Safety. *Adv. Civ. Eng.* **2021**, *2021*, 1−13.

(4) Zeng, J.; Tian, S.; Wu, G.; Zuo, Y.; Xu, S.; Pei, P.; Wang, C. The Research of Coal Seam Gas Pressure and Initial Gas Emission Characteristics of Borehole. *Energy Sci. Eng.* **2019**, *7*, 1961−1969.

(5) Shi, X.; Song, D.; Qian, Z. Classification of Coal Seam Outburst Hazards and Evaluation of the Importance of Influencing Factors. *Open Geosci.* **2017**, *9*, 295−301.

(6) Skoczylas, N. Coal Seam Methane Pressure as a Parameter Determining the Level of the Outburst Risk - Laboratory and in Situ Research/Ciśnienie Złożowe Jako Parametr Określający Stan Zagrożenia Wyrzutami Metanu I Skał - Badania Laboratoryjne I Kopalniane. *Arch. Min. Sci.* **2012**, *57*, 861−869.

(7) Wei, C.; Zhang, L.; Hao, M.; Nie, Y.; Wang, R. Discrimination Method of Gas Pressure Measurement in Coal Seams: Physical Experiment and Model Development. *ACS Omega* **2022**, *7*, 30412−30419.

(8) Cui, X.; Zhang, J.; Guo, L.; Gong, X. A New Method for the Measurement of Gas Pressure in Water-Bearing Coal Seams and Its Application. *Geofluids* **2020**, *2020*, No. e8881063.

(9) Zheng, W.; Yang, S.; Ma, W.Analysis of Factors Affecting the Measurement of Coal Seam Gas Pressure *Saf. Coal Mines* 2009; Vol. *40*, pp 82−84.

(10) Lan, Z.; Qu, R.; Chen, X.; Liang, W.; Qi, L.; Bai, S.Current Situation and Analysis of Direct Method for Measuring Coal Seam Gas Pressure *Saf. Coal Mines* 2009; Vol. *40*, pp 74−78.

(11) Tian, J.; Xie, H.Analysis of Factors Influencing Coal Seam Gas Pressure by Indirect Method *Coal Technol.* 2018; Vol. *37*, pp 206−207.

(12) Wang, S. Study the Sealing Pore Technique of the Nearly Horizontal Gas Drainage Hole In-Seam *IOP Conf. Ser.: Earth Environ. Sci.* 2019; Vol. *358*032013 DOI: 10.1088/1755-1315/358/3/032013.

(13) Sun, Z.; Li, X.; Wang, K.; Wang, F.; Chen, D.; Li, Z. Determination of Key Technical Parameters in the Study of New Pressure Sealing Technology for Coal Seam Gas Extraction. *Int. J. Environ. Res. Public Health* **2022**, *19*, 4968.

(14) Li, J.; Zhao, Y.; Du, J. Prevention Technology of Coal Spontaneous Combustion Induced by Gas Drainage in Deep Coal Seam Mining. *Fire* **2022**, *5*, 65.

(15) Zhou, D.; Wang, X.; Guo, C.; Zhou, J.; Wang, K. Research and Application of Hydraulic Fracturing Borehole Bag Sealing Technology. *IOP Conf. Ser.: Earth Environ. Sci.* **2021**, *781*, No. 022008.

(16) Yu, S.; Su, X.; Song, J.; Wang, Q.; You, Z. The Hole Sealing Technology of Solid−Liquid Materials with Three Pluggings and Two Injections for Gas Extraction Hole in the Coal Mine. *ACS Omega* **2022**, *7*, 43847−43855.

(17) Xiong, W. Comparative Analysis of Sealing Effect of Different Hole Sealing Processes in Coal Mine. *J. Phys.: Conf. Ser.* **2021**, *2005*, No. 012205.

(18) Chao, Z.; Zeng, X.; Jiang, B.; Zhai, C.; Zhu, C.; Ni, H. Experimental Study on Mechanical Behaviour and Pore Evolution of Borehole-Sealing Materials under Different Confining Pressures. *Arab. J. Geosci.* **2022**, *15*, 310.

(19) Qin, W.; Xu, J. Dynamic Secondary Borehole-Sealing Method for Gas Drainage Boreholes along the Coal Seam. *Geofluids* **2018**, *2018*, 1−11.

(20) Song, Y.; Bao, R.; Shi, B. Experimental and Theoretical Study of the Time-Effect-Based Instability Characteristics of the Gas Drainage Borehole Sealing Section in a Soft Coal Seam. *ACS Omega* **2022**, *7*, 9303−9309.

(21) Zhang, J. F.; Chen, X.; Liu, Y.; Zhang, H.; Wang, C.; Fang, G. Investigation on Grouting Diffusion in Inclined Fracture with Flowing Water Conditions. *Arab. J. Geosci.* **2022**, *15*, 629.

(22) Zhao, D.; Pan, J. Numerical Simulation on Reasonable Hole-Sealing Depth of Boreholes for Gas Extraction. *AIP Adv.* **2018**, *8*, No. 045003.

(23) Zhang, W.; Wu, F.; Han, C.; Li, X.; Peng, Z.; Ren, Q.; Yang, F.; Zhang, D. Criterion of Grouting Pressure in Regional Advance Grouting Treatment to Prevent Water Disaster from Karst Aquifers in Coal Seam Floors. *ACS Omega* **2022**, *7*, 29274−29286.

(24) Zhang, G.; Yuan, S.; Sui, W.; Qian, Z. Experimental Investigation of the Pressure and Water Pressure Responses of an Inclined Shaft Wall During Grouting. *Mine Water Environ.* **2020**, *39*, 256−267.

(25) Ma, X.; Zhang, L.; Zhou, J. Experimental Study on the Relationship Between Grouting Pressure and Compressive Strength of Hardened Cement Paste. *Iran. J. Sci. Technol., Trans. Civ. Eng.* **2020**, *44*, 483−489.

(26) Yi, L.; Yu, Q.Numerical Simulation of Plastic Zone Around Densely Drilled Holes Changing with Coal Strength *Min. Saf. Environ. Prot.* 2008; Vol. *1*, pp 1−3.

(27) Fiorillo, F.; Esposito, L.; Leone, G.; Pagnozzi, M. The Relationship between the Darcy and Poiseuille Laws. *Water* **2022**, *14*, 179.

(28) Wei, J.; Yao, B.; Liu, Y.; Wang, D.; Cui, P.; Yao, S.Grouting Fluid Diffusion Law and Variable Mass Seepage Model for Fractured Coal *J. China Coal Soc.* 2020; Vol. *45*, pp 204−212.